

Telescopes as Mechatronic Systems

Hans Jürgen Kärcher

Abstract— The system design of telescopes is usually dominated by the aspects of the optics and receiving instruments. The telescope structure, mechanic and control are “only” aids to position these elements to the celestial target, but their quality has a big impact on the final performance. The paper describes an integrated design approach to these “mechatronic” telescope subsystems.

I. INTRODUCTION

The construction of optical telescopes in former times was dominated by the problem of manufacturing and shaping the optical surfaces. The construction of the first large radio telescopes was dominated by the problem of designing and manufacturing the deformation stable reflector backup structures. Currently, these issues (see ref. [1] and [2]) no longer dominate the telescope design. The telescopes are understood as integrated systems, where all contributing engineering disciplines, as optics, structural mechanics, control, civil engineering, as well as management and commercial aspects, have the same impact during the design, construction and operational periods. One major subgroup is the mechanical and control subsystem, here called “mechatronic” subsystem. This paper describes the mechatronic aspects of telescopes from the viewpoint of structural mechanics, with focus on structural design, axes mechanisms, active surfaces, sensor placement, and system identification with application to the surface and pointing control. The issues are highlighted by latest examples of actually built optical and radio telescopes.

II. SYSTEM ASPECTS OF TELESCOPE DESIGN

Purpose of a telescope is to observe astronomical objects on the sky. Therefore it consists of (Figure II-1) reflectors¹ and receivers, and a structural, mechanical and control system, which points these elements to the celestial target. The wavelengths, at which the receivers are used, define the required accuracies for the reflector surfaces and pointing, and thereby the requirements for the structural, mechanical and control system. The accuracies are challenged by telescope inherent properties, such as manufacturing errors,

friction etc., and by environmental influences, as gravity, wind, and temperature. The mechanical system consists of a structure, which supports the optical elements, and the main axes drives, which control the position on the sky (see [1]). Modern telescopes have additional actuators and sensors, which control internal deformations (Figure II-1). The integrated design of these elements, structure, actuators, sensors and controllers is subject of this paper.

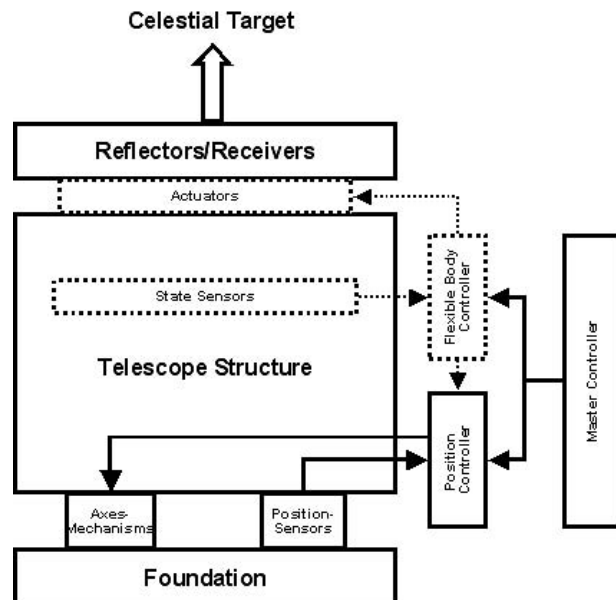


Figure II-1 System architecture of a telescope with deformation control features

III. STRUCTURAL DESIGN

The structure is the “backbone” of all other systems. In previous times, some remarkable special design features for telescope structures were developed to fulfill the accuracy requirements of the optical elements in a passive, “structural mechanics” way. Examples are the Serurier-struts for the tube of optical telescopes, the iso-static supports of optical mirrors, the equivalent “homology” principles for backup structures of radio reflectors, or the use of high tech materials as glass ceramics or carbonfiber composites. With the upcoming active and adaptive optics, as some system designers argued, the structural design issues may be less important, because the active systems may have the potential to compensate all the unwanted influences of the struc-

H.J. Kärcher is with MAN Technologie AG, 55024 Mainz, Germany (e-mail: Hans_Kaercher@mt.man.de).

¹ For optical telescopes, the reflectors are called „mirrors“.

ture. This reasoning is not acceptable. The aim of ultimate performance can only be reached by ultimate design of all subsystems, including the structure, not to mention that a structural improvement can be cheaper and more reliable than the active compensation. And integrated design includes – at least – understanding the principles of structural design.

Figure III-1 shows, for example, two alternate structural design concepts for EL/AZ mounts, the left one with the central support of the reflector backup structure between the two elevation bearings, the right one with an external support and open space between the elevation bearings. The choice between the two concepts has a great impact on the arrangement of receiver equipments, as well as on the deformation behavior of the overall system. Details are described in [1] and [3].

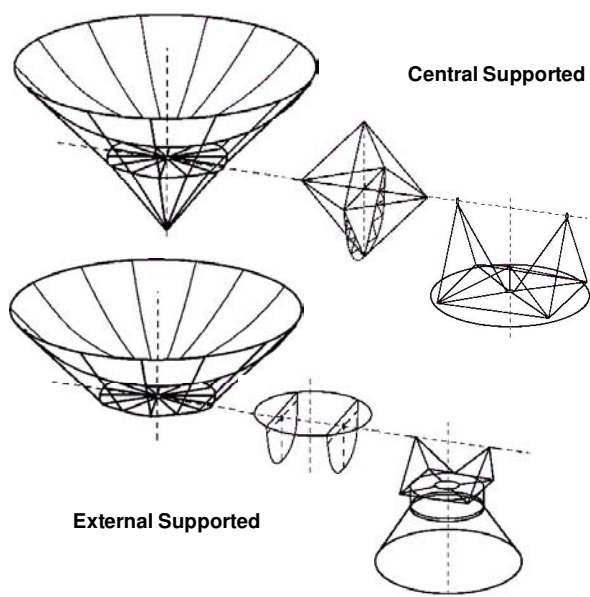


Figure III-1 Alternate structural concepts for Elevation over Azimuth mounts

IV. AXES MECHANISMS

For the basic positioning of the telescope on the sky, the telescope masses must be moved with respect to the azimuth and elevation axes. The axes mechanisms consist of two major elements, a bearing and a drive mechanism. Here is a list of comments on the mechanical design of these two elements:

§ For smaller and mid-sized telescopes the azimuth bearing is typically a single, vertically oriented roller bearing of a large diameter. For large telescopes, it may be split into a wheel-on-track arrangement for the vertical loads, and a central pintle bearing for the horizontal loads (see e.g. [4], [5]).

§ The elevation axis includes typically two separate, horizontally oriented roller bearings of small diameter.

§ Large optical telescopes use often hydrostatic bearings instead of roller bearings. Main argument for hydrostatic

bearings is low bearing friction and its reduced influence on telescope pointing.

§ The drive mechanism consists normally of mechanical reducers as planetary gear trains, meshing via pinions into a gear rim on the axis. For the wheel-on-track case, the drive mechanism acts directly on the wheels (friction drive)

§ Driving torque is articulated at the input shaft of the gearboxes by modern AC or DC torque motors.

§ Backlash of the gear trains can be suppressed by biasing two or more gear units per axis.

§ Large optical telescopes use nowadays backlash-free direct drives.

§ Additional standard features for the drive mechanisms are limit switches, brakes, stow mechanism, emergency drives etc.



Figure IV-1 Examples of axes mechanisms

V. POSITION CONTROL

A. Standard Concept with Mechanical Reducers

Standard position control system is a cascade control concept (Figure V-1). It consists of fast inner loops for the motor currents (bandwidth > 1000 Hz), medium speed control loops for the motor velocities (bandwidth > 50 Hz), and slow position control loops (bandwidth < 1 to 10 Hz). It includes the conventional PID controllers, and is in practice very stable and robust. Its limits are as follows:

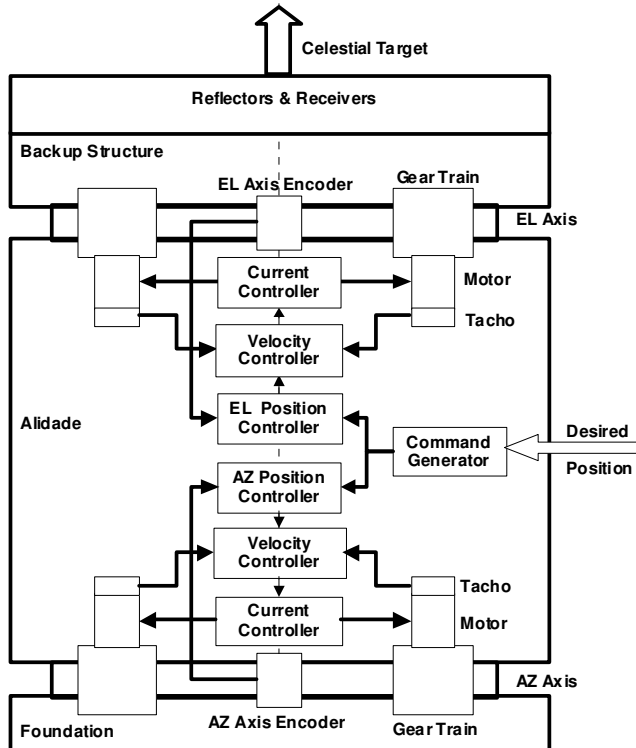
§ The bandwidth of the position loop is limited by the lowest natural frequency of the telescope structure and cannot be increased without exciting structural resonance

§ The position sensors (= main axes encoders) measure only the relative movement at their attachment flanges. De-

formations of the structure beyond the attachment flanges are out of influence of the position control loops.

§ Friction in the bearings and gear trains is an issue, if the pointing requirements are high. Friction was the main argument for using for the mechanical axes concepts hydrostatic bearings instead of roller bearings.

§ Modern torque motors, compact and digital controlled allow the reduction of the gear ratios in the gear trains com-



pared with analog controlled motors (gear ratios < 100 instead of > 50.000)

Figure V-1 Standard cascaded main axes control architecture

B. Direct Drive Concept

Direct drives avoid the need for mechanical reducers. Motors with high torque capability are directly attached to the axes. Change of the “classical” control concept to the “modern” direct drive concept has for large telescopes the following implications:

§ Friction and backlash implied by the gear trains is completely eliminated (main advantage of the direct drive).

§ The mechanical compliance of the gear trains between the motor action and the reaction of the structure is eliminated. The motors have a much more direct influence on the structure, and may excite unwillingly higher resonance modes.

§ The motors can be used much more effectively for compensating disturbances.

§ The additional standard equipment as limit switches, brakes, safety devices etc. are very different to the classical drive concept using gear trains and must be adequately adapted to this alternate concept.

§ Up to now no experience with direct drives for large telescopes > 12 m reflector diameter exists.

Conclusion: The current and future telescope drive will use the classical main axis concept (with biased gear trains of low gear ratio, but upgraded with modern AC or DC torque motors) and cascaded control architecture. Direct drive concepts may be restricted to smaller telescopes with high positioning accuracy requirements.

VI. FLEXIBLE BODY CONTROL AND ADAPTIVE OPTICS

The classical position control as described in the previous chapter could be in principle executed without deeper knowledge of the structural and mechanical behavior. The only limits to be known to the designer are the lowest natural frequency, and the limits of backlash and friction in the gear trains. In contrast to this “simple” approach, “Flexible Body Control” (FBC) is understood as taking into account the knowledge of the deformation of the telescope structure in the design of the control loops.

FBC can be achieved by different system engineering methods:

1. FBC using the existing information of the classical control system for understanding the structural deformations and related adaptation of the controllers.
2. FBC based on information from state sensors on the telescope structure.
3. FBC based on information of external metrology systems, such as laser rangars.
4. FBC based on information of imaging sensors in the focal plane of the telescope.

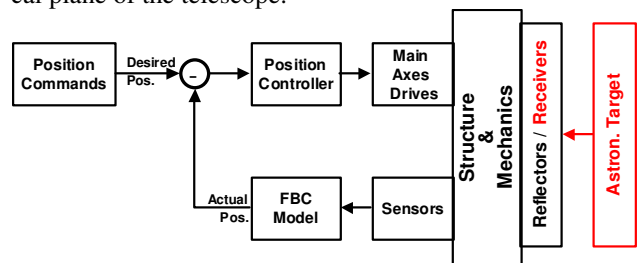


Figure VI-1 Basic FBC Control Architecture

Figure VI-1 shows the simplest approach, using the sensors in the typical control system (the position encoders, the tachometers and the motor current sensors) for compensating the influence of structural deformations on the pointing. Simplest example is the compensating of the gravity deformations of the reflector backup structure as a function of the elevation angle by look-up-tables derived from finite element calculations in an open loop manner.

Figure VI-2 shows an approach based on the state sensors on the telescope structure. These could be temperature sensors, inclinometers, accelerometers etc. (for more details on sensors see chapter VII). The additional information can be used to compensate not only pointing deviations, but also deformations of the reflector itself. But for this purpose, additional actuators for correcting the surface are needed (for more details on active surface see chapter X).

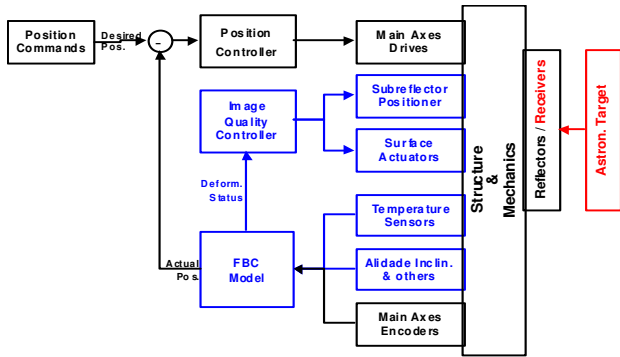


Figure VI-2 FBC Control Architecture Details

The FBC concept with the state sensors depends completely on the quality of the FBC-model, which extrapolates the deformations from the measurement data. The FBC-model may use algorithms similar to those used for system identification in modal survey testing (see chapter VIII). The FBC model has to separate the overall pointing deformations and active surface corrections. The state sensor method is also an open loop approach method.

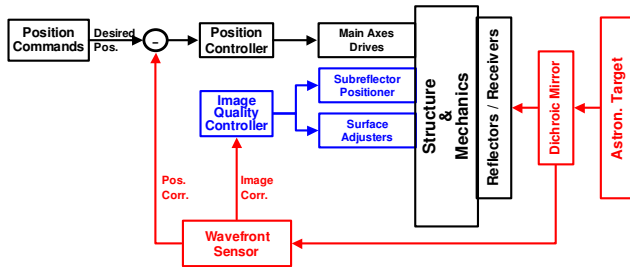


Figure VI-3 FBC based on wave front sensor in the focal plane

Figure VI-3 shows the ultimate FBC concept in the closed loop approach, with a wave front sensor in the focal plane of the telescope. Wave front sensors depend on the observation of reference stars, and are available only for optical telescopes. For applications in radio telescopes, up to now, no adequate wave front sensors have been developed. The wave front sensor as shown in Figure VI-3 does not distinguish between disturbances caused by the telescope itself and those caused by the atmosphere. Therefore the concept is used for optical telescopes also to compensate atmospheric blur and is called “adaptive optics” (see chapter X).

VII. DEFORMATION SENSORS

Figure VII-1 gives a list of all kinds of sensors from which information on the deformation state of the telescope can be extrapolated. Their purposes, pros and cons are discussed in this chapter.

	Sensor Type	Kind of Information	Main Application
a	angular encoders	relative angular position of adjacent structural components	position control of earthbound telescopes
b	tachos	motor velocities	
c	current sensors	motor torques	
d	inclinometers	inclination of attachment flange against local gravity	FBC for radio telescopes
e	laser trackers	relative spatial position of target points	
f	temperature sensors	absolute temperature	
g	pressure sensors	aerodynamic pressure at attachment area	
h	strain gauges	strain at attachment area	
i	imagers	position of a reference target	position control and FBC for airborne (and space) telescopes
j	gyros copes	angular accelerations	
k	accelerometers	lateral accelerations	adaptive optics
l	wave front sensors	image and position of a reference target in the focal plane	
m	weather stations	wind speed, wind direction, outside temperature etc.	

Figure VII-1 Sensors types used as deformation state sensors

A. Position control sensors for earthbound telescopes and their possible use for FBC purposes

a) Angular encoders are the standard position sensors in the typical position control. There are extremely precise encoders available from renown vendors. In their implementation, their attachment requirements (large through holes on the axis) must be taken into account (Figure VII-2). Direct attachment on the axis without need for additional couplings should be preferred for applications with high accuracy requirements. Also, it should be always considered that the angular encoders measure the relative angular positions at their attachment points, and the deformations of the overall structural system may influence the overall precision.

Essential aim of the angular encoders is the measurement of two relative rotations of the two main telescope components (elevation and azimuth) in the sense of rigid body movements. Their main contribution to flexible body control could be the identification of the gravity deformation in elevation, and using them for compensation in lookup tables (as a function of the elevation angle).



Figure VII-2 Attachment variants of encoders²

² Figures from Heidenhain leaflet

b) Tachometers on the motor axes are always needed in the cascaded control loop concept for the fast control of the motor speed. They are also perfect for the synchronization of the “more than one drive per axis systems” and for the related backlash-compensation features. Their measurement principle is that of an AC generator.

c) Current sensors are needed for the fast control of the motor currents, and can be thereby used for the evaluation of the motor torques. In the sense of flexible body control, they give an information on the magnitude of the wind forces, against which the motor torques act, and can be used for respective compensation algorithms (see chapter VIII and XI).

B. FBC sensors for radio telescopes

d) Inclinometers are the first sensors in this list, which may be added only for the FBC purposes. They are very accurate (0.1 arcsec or better); the problem is the right location on the structure, and the dynamic tuning into the control loops. They are predestinated for measuring the misalignment and disturbances of the azimuth axis and the alidade at the elevation bearings (see Figure VII-3 and [8]). They can be used for estimating the overall deformation state of the telescope under wind load in the sense of “modal observers” (see [7] and chapter VIII).

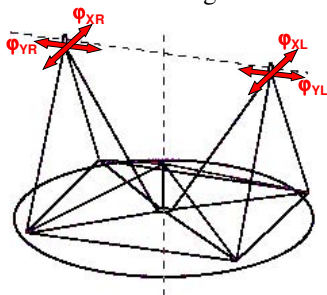
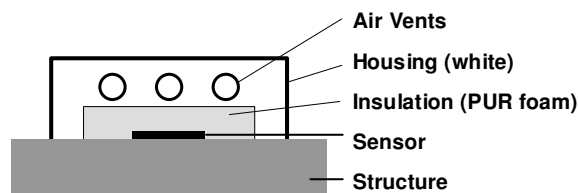


Figure VII-3 Inclinometers on the alidade in the vicinity of the elevation bearings

d) Laser trackers are used in some large telescopes as source for active surface control (see e.g. [10]). Laser trackers measure the position of dedicated target points in sequential manner in three coordinates. Laser trackers are “external” means like wave front sensors. Their measuring data can be used for closed loop corrections, and do not need internal knowledge of the causes for the deformations. They are obviously powerful tools (see the bibliography in [10]), but here not further discussed, because their use is contrary to the “mechatronic approach”, which is the focus of this paper, and may lower demands in the structural design.

Figure VII-4 Attachment concept for temperature sensors

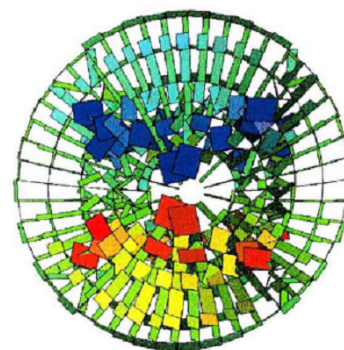


e) Temperature sensors on the structure are the first choice for flexible body control of temperature effects on telescope structures, and are widely used (e.g. [6], [8], [10]).

They need a careful application to measure actual temperature of the structure at the attachment point, and not the temperature of the surrounding air (see Figure VII-4, taken from [6]). For the evaluation of pointing and surface corrections, an estimate of the temperature induced deformation state is needed, which can be based on interpolation of the measured temperatures on the structure, and a finite element calculation of the related deformations. Temperature variations are normally very slow. Therefore, the corrections can be introduced into the FBC control loop in form of lookup tables (see chapter XIV).

Figure VII-5 Strain distribution in a reflector backup structure under gravity load

f) Strain gauges could be used similarly to the temperature sensors for the identification of deformation states under external loads, and their application on the structure needs similar caution.



For the evaluation of the overall deformations from the individually measured strains, an extrapolation algorithm is needed (e.g. modal observers see [7] and chapter X). Due to the large number of structural members, and the complexity of the strain distribution (see example in Figure VII-5, taken from [7]), this task is not trivial, and up to now no real application is known to the author.

C. Position control and FBC sensors for airborne (and space) telescopes

Airborne and space telescopes have, compared with earthbound telescopes, no stable reference in the form of a foundation for “blind” pointing of the telescope on the sky. To find the absolute position in the sky, they must rely on imagers observing reference stars with known celestial position. For position stability they use their own mass as basis (inertial stabilization). The following comments are based on the experience of the author with the airborne telescope SOFIA. For space telescopes, the principles may be the same, but the environment is quite different. The airborne telescope is exposed to a very harsh dynamic environment, where FBC concepts also for the control of higher frequent excitations are absolutely essential.

g) Imagers are a simple wave front sensor used to observe the celestial position of known reference stars. In some areas of the sky, only faint reference stars may be available, and therefore the imagers may be slow, and not suitable for fast position control.

h) Gyroscopes measure angular accelerations. In their modern, fiber optic version (see [16]) they are rather robust and have a high sensitivity. The relative position can be

obtained by two-fold integration. Together with a focal plane imager, they substitute the main axes encoders of the earthbound telescopes.

i) Accelerometers are widely used in structural dynamics for system identification based on modal survey tests (see e.g. [12]). They are applicable for the identification of dynamic effects, and they are very effective, and a lot of experience is available from modal survey applications. For the application in the SOFIA telescope (Figure VII-6), the practical restrictions of the attachment of the accelerometer/gyro unit onto the structure (on the cabin side of the telescope) require the identification of the deformation state during operation. FBC algorithms are used for the separation of the influence of gravity deformations, low frequent flight maneuvers, and higher frequent aero-acoustic excitations (see [13], [14], [15]). As an additional obstacle, the main axes of inertia of the telescope are slant to the optical and main drive axes.

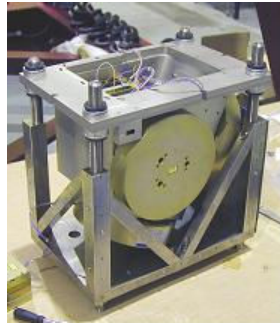


Figure VII-6 Three-axis accelerometer/gyro unit of the airborne telescope SOFIA

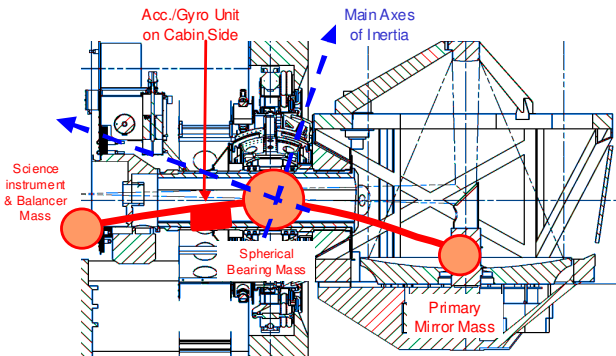


Figure VII-7 Location of the accelerometer/gyro unit and orientation of the main axes of inertia of the airborne telescope SOFIA

D. Sensors for Optical Telescopes

j) Wave front sensors are widely used for optical telescopes under the headline “adaptive optics” (see e.g. [17]). Their main purpose is the compensation of atmospheric blur caused by air turbulence in the beam path of the telescope. Adaptive optics makes earthbound telescopes competitive to space telescopes. The upcoming extreme large optical telescopes with mirror sizes up to 100m would not be feasible without adaptive optics. Instead of a natural reference star on the sky, as used in SOFIA, adaptive optics is based on artificial reference stars (see [18], Figure VII-8). The image of the artificial star is used to get information for position as well as image corrections. The wave front sensor does not distinguish between disturbances caused by the

atmosphere against disturbances caused by the telescope optical and mechanical systems.

Adaptive optics approach is fascinating and opens new areas for astronomical observations. Nevertheless, the implementation should be accompanied by the development of a telescope mechatronical subsystem of similar excellence. Therefore, for the underlying structural, mechanical and control subsystem of the future extreme large telescope, the mechatronical approach, as described above for the large radio telescopes, should be developed appropriately.

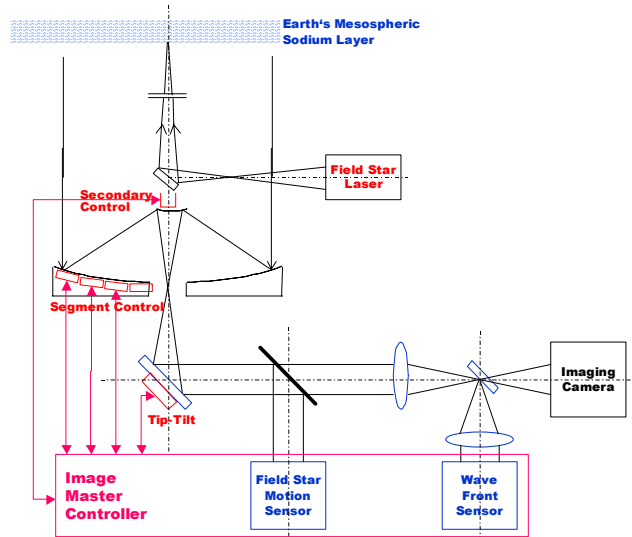


Figure VII-8 Wave front sensor based on artificial stars³

VIII. SYSTEM IDENTIFICATION

All sensors as described in chapter VII give only state data at the locations which they measure. For the evaluation of the overall deformation of the telescope, some kind of extrapolation of the measurement data is needed. This chapter gives a basis for the selection of extrapolation algorithms⁴. The best tool for representing the deformation behavior of the telescope is a finite element model, which includes the structure and drives (e.g. Figure VIII-1). The model includes the attachment points of the sensors, and the overall deformation behavior can be analyzed, if the loads causing the deformations are known.

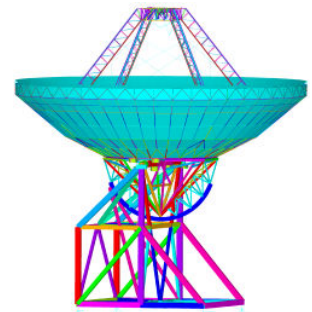


Figure VIII-1 Overall finite element model of a large radio telescope⁵
Wind is a major source for deformations of a large exposed radio telescope, and the distribution of wind loads on the telescope structure as a function of the elevation angle and

³ according [17]

⁴ “Nothing is more practical than a good theory”.

⁵ 64m SRT Sardinia, Italy

the angle of attack are known from wind tunnel test data. Based on this load data, the related deformations can be calculated as well as the nominal state data at the attachment points of the state sensors. Correlating the necessary correction data e.g. for the pointing deviations with the sensor data gives the needed information for the corrections via the FBC controller as described in chapter VI. It is shown in [8], that four inclinometers arranged as sketched in Figure VII-3, for the 50m radio telescope LMT in Mexico, improve the pointing accuracy under quasi-static wind by a factor of 10. Similar improvements can be achieved with temperature sensors and a correction model developed in a similar manner (e.g. the temperature sensors on the alidade of the 32m Merlin telescope in Cambridge, UK, see [6]).

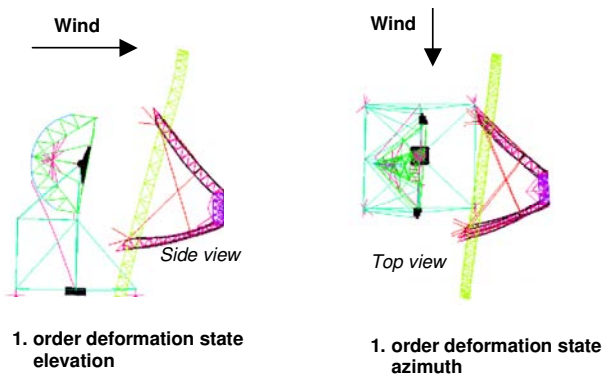


Figure VIII-2 The two “principle” first order deformation states of a radio telescope

The described extrapolation algorithms are – from a general point of view – in so far unsatisfactory, as they depend on assumptions of the knowledge of forces causing the deformations.

Figure VIII-2 shows two “principle” deformation states of a telescope in horizontal position (one symmetrical correlated to deviations in elevation, and one anti-symmetrical correlated to deviations in azimuth). These deformations could be caused by wind as indicated in the sketch, but could be also caused by the main axes drives. This suggests the development of the deformations into a series of mode shapes obtained from the modal analysis (see [7]). This “modal observer” approach has the advantage of being independent of load

IX. POINTING CALIBRATION, OPTICS

Active surface control is discussed in the following chapter. Before discussing this, some remarks to “pointing calibration” and “optics” are introduced.

It is good practice, to “calibrate” radio telescopes pointing regularly before observations [20]. The method uses an “astronomical” pointing model independent from the design data of the telescope. It is based on the observation of known celestial targets and may include corrections of atmospheric effects by weather data [19]. Figure IX-1 shows

the control architecture that includes pointing calibration feature.

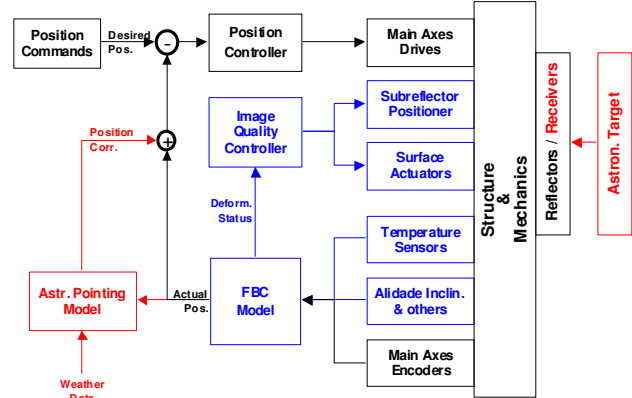


Figure IX-1 FBC control architecture including an astronomical pointing calibration model

The correlation between the pointing calibration model and the system identification by the FBC model includes some understanding of the “optics” of the telescope. Figure IX-2 shows some principal features.

The position of the deformed reflector surface, e.g. under gravity influence as indicated in the figure, deviates from the nominal position as defined by design drawings or reference marks. For optical telescopes, the deformations influences can be analyzed by “ray-tracing” algorithms⁶.

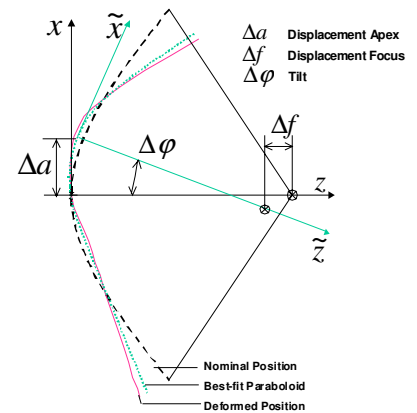


Figure IX-2 Best-fit position of a deformed reflector

For radio telescopes, with their normally “1 pixel” field of view, a simplified ray-tracing approach is based on best-fitting of Zernike polynomials for the reflector surface, and a complementing by the “pointing formula”, describing the influence of subreflector deviations (see [3]). The position and surface corrections are implemented into the overall control system inside the block of “FBC model” and “image quality controller” of Figure IX-1.

For the influence of the optical layout on the overall structural, mechanical and control design of telescopes see [1], [2] and [3].

⁶ Commercial software packages are available (e.g. GRASP8, TICRA engineering consultants, Copenhagen, Denmark, www.ticra.com)

X. ACTIVE AND ADAPTIVE SURFACES

In regard of the actuators in the control loops, up to now only the main axis drives were discussed (chapter IV). In this chapter, the design features of the actuators of the active surfaces itself are commented. The design of these actuators is related to the partitioning of the reflector into individual panels. Figure X-1 shows on the left a hexagonal partitioning, which is typically used for large optical telescopes, and on the right a radial-circumferential partitioning, which is used for large radio telescopes. The shape and size of these panels is chosen by consideration of manufacturing aspects.

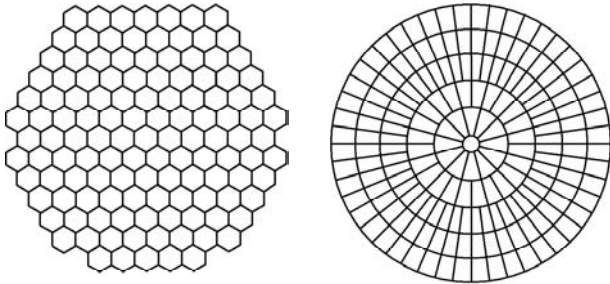


Figure X-1 Partitioning of telescope reflectors into hexagonal (left) or radial-circumferential (right) panels

The Euro50 extreme large optical telescope concept [21] e.g. uses hexagonal mirror segments of 2m size, which results into 618 mirror segments for the overall 50m reflector. The 50m LMT radio telescope [8] uses panel units of 2.5x5m size, which results into a total number of 180 panel units. These panel units are supported by the reflector backup structure (BUS), and the interface between the panels and the BUS define the locations where the actuators of the active surface should be placed.

A. Surface Actuators for Radio Telescopes

Radio telescopes need only slow surface corrections. Therefore, the actuators can be based on planetary screws with low pitch, driven by torque motors Figure X-2. The corners of adjacent panels are driven together by one shared actuator. The structural coupling is done by adjusters, which are aligned during the installation of the panels. The adjusters should have some lateral flexibility preventing unforeseen lateral constraints.



Figure X-2 Surface actuators of the 64m SRT (left)⁷ and the 15m IRAM (right) telescopes

⁷ from [22]

B. Optical Telescopes

The hexagonal segments of extreme large optical telescopes may need fast control. Therefore, in Figure X-3 the actuators are subdivided into two units, a slow one, which could be of screw type similar to that described for the radio telescopes, or hydrostatic or pneumatic as usually for optical mirrors, and additionally a fast actuators with a reaction mass feature. The fast one may be based on voice coil or direct linear drive principle. The reaction masses prevent the transfer of higher frequency dynamic reactions to the BUS structure, needed to reach the challenging optical performances in a wind exposed environment

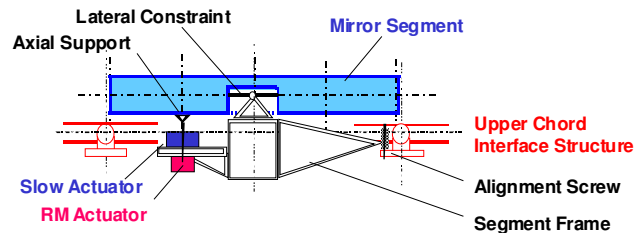


Figure X-3 Actuator concept for hexagonal mirror segments

Figure X-4 shows the control architecture, which separates the function of the slow and fast actuator. The slow actuator is responsible for the position of the mirror segment in the overall mirror system, and depends from the position input of the overall image quality sensor. The fast reaction mass loop is independent from external influences and relies only on the information from the local accelerometers complemented by disturbance feed forward of wind fluctuations identified by pressure sensors.

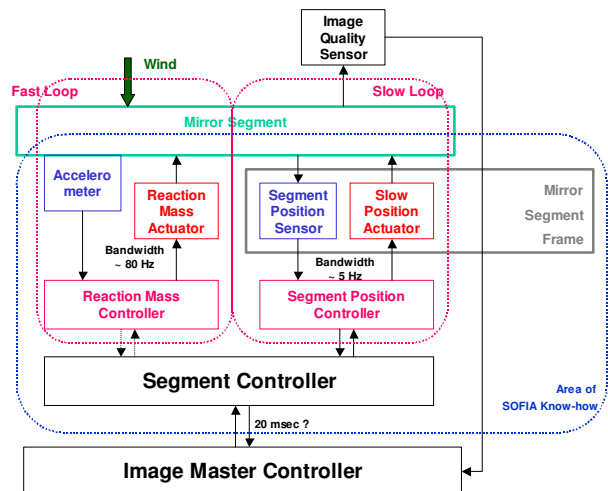


Figure X-4 Control architecture for the reaction mass actuators

The described concept reflects experience in the SOFIA project. Figure X-5 shows the SOFIA mirror cell (whiffle tress, carbonfiber structure) with prepared attachment points for reaction mass actuators. The concept was studied in detail [23], the decision on the application will be made after test of the aeroacoustic environment inside the aircraft cavity. The first test flights will be in 2005.



Figure X-5 SOFIA 2.7m mirror cell with attachment points for reaction mass actuators

C. Subreflector Positioner and Wobbler

Additionally to the active control of the main reflector position and shape, also the position of the subreflector is actively controlled. Additionally, the millimeter radio telescopes and infrared telescopes require often a wobbler for fast observation of background radiation in the vicinity of a celestial target.



Figure X-6 Subreflector positioner (left) and wobbler (right) of the 30m MRT Spain

A hexapod type actuator system is the universal device for slow (“steady-state”) positioning of the subreflector (e.g. Figure X-6 left). It allows the alignment in all six rigid-body degrees-of-freedom. For the fast wobbling, a dynamically balanced reaction mass system is needed (e.g. Figure X-6 right).

D. Adaptive Secondary or Tertiary Mirrors

For optical telescopes with monolithic primary mirrors, the active/adaptive correction of the incoming wave front is usually realized by an active mirror in the beam path behind the secondary mirror (“active/adaptive tertiary”). Sometimes the secondary itself has active surface features [24]. Also subreflectors for radio telescopes with active surface are built.

XI. END-TO-END SIMULATION

Final tool for optimizing the telescope as a mechatronic system is the end-to-end simulation of all subsystems with focus on the pointing accuracy due to disturbing effects that define the ultimate performance. In the chapters above, an overview on all the subsystems was given. What is missing (before the execution of the end-to-end simulation) is the description of the external disturbances. These are mainly environmental influences as gravity, wind, temperature, and unavoidable internal effects as vibrations induced by subsystem aggregates, friction and command disturbances. All the disturbances may have a steady-state component and dynamic components.

A. Simulation of steady state effects

Simulation of steady-state effects has a long tradition. In our days, it is based on finite element models of the overall system (see e.g. Figure VIII-1).

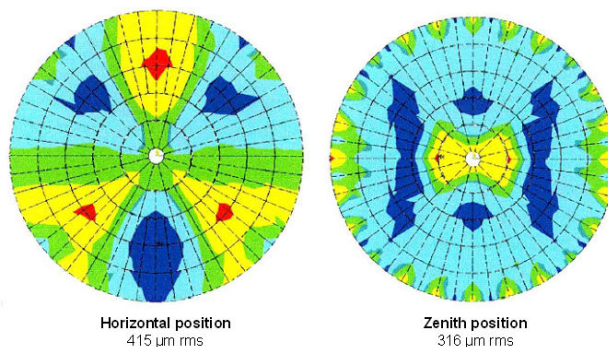


Figure XI-1 Main reflector deformation patterns (gravity 50m LMT)

The loads for calculation of the major environmental influences are gravity loads (from the design drawings and parts lists of all components), wind loads (from wind tunnel test data), and temperature loads (from a thermal model, see chapter XII). Figure XI-1 shows typical deformation patterns, obtained from the finite element calculations and evaluated with the best-fitting post-processor. The data from these figures are typical inputs for the active surface error compensation via the surface actuators of Figure X-2 and lookup tables in the FBC system of Figure VI-2.

B. Simulation of dynamic effects in the time domain – radio telescopes

Recently powerful tools for the simulation of dynamical effects are available⁸, which are used for the simulation of the influence of wind gusts on the telescope pointing performance. Core of the end-to-end model is a modal representation of the finite element model. The finite element model itself is too large to be used in the full size end-to-end model. The latter comprises simulation blocks for the wind loads, the ray-tracing (pointing error model), the sensor readings, the drive torques and the position controller itself.

⁸ e.g. MATLAB/SIMULINK, www...

Largest model uncertainty is in the wind load modeling (see e.g. [25]).

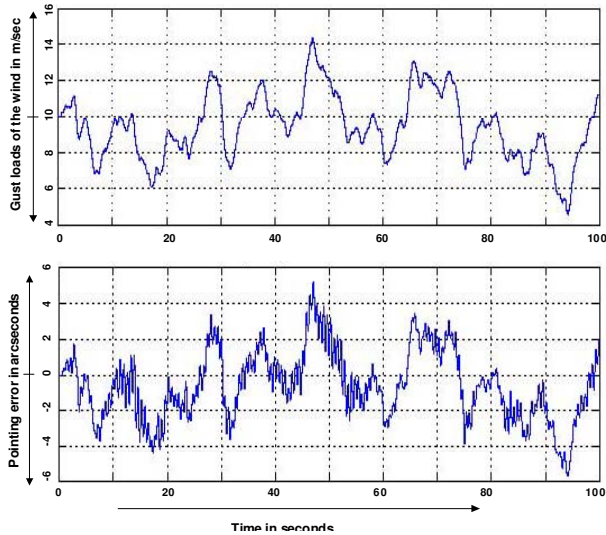


Figure XI-2 Simulation results of the influence of wind gusts on a radio telescope

The results in Figure XI-2 show a good correlation of the motor torques with the wind load input, which could be the bases for the correction of the slower components of the wind induced pointing errors (see [26]).

C. Simulation of dynamic effects in the time domain – airborne optical telescope SOFIA

The simulations of dynamic effects on radio telescopes show that most of the influences can be handled in the low frequency, or steady-state domain. Higher frequency effects are mostly ignored and compared with the requirements (this statement assumes that no major design flaws are made in the structure, and the control system). The situation is different for the airborne telescope SOFIA. The simulation results (e.g. Figure XI-4) for this telescope give some insight into the higher frequent effects.

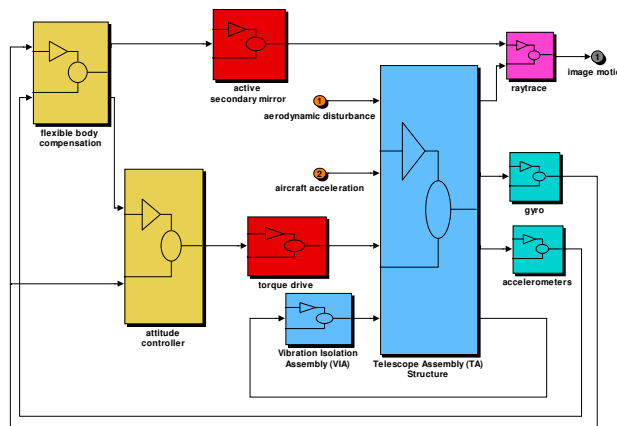


Figure XI-3 End-to-end simulation model for the airborne telescope SOFIA

The end-to-end simulation model for SOFIA (Figure XI-3) comprises a FBC model for the active correction of the pointing via the fast secondary mechanism. The flight disturbances are introduced into the model by time histories of aero-acoustic pressures, measured in wind tunnel tests of the telescope in the open cavity of the aircraft [27]. The aircraft vibrations are obtained from the measurements at real Boeing 747SP aircraft

The simulation results for the SOFIA pointing are plotted in Figure XI-4 as a function of the frequency. There are different dynamic ranges. In the “servo domain” up to 25 Hz, the system is controlled, by the main axes drives from 0 to 10 Hz, and above by the active secondary. Above 25 Hz no active control system is assumed, and the behavior is dominated by structural dynamics. The main influences on the cumulated errors are related to structural resonance (“dumbbell”, “rocking” modes) and aero-acoustic (“organpipe” modes) .

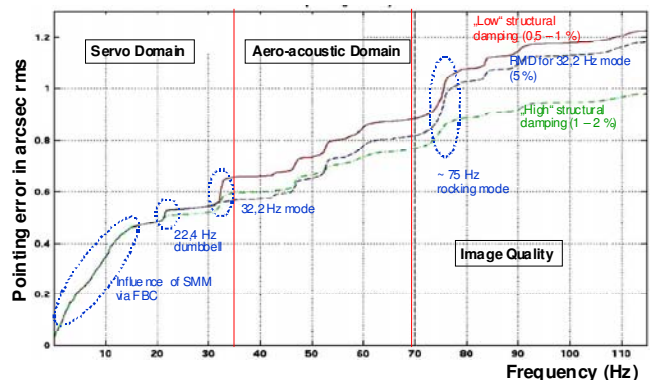


Figure XI-4 Simulation results – cumulated pointing errors for the airborne telescope SOFIA

D. Earthbound Optical Telescopes

Optical telescopes are traditionally built inside a dome, which protects them against the weather conditions. During operation only a small section of the dome was opened to prevent wind influences. In the last decades, larger exposure of the telescopes to wind during operation was allowed, mainly to improve the “dome seeing” by natural convection. For the investigation of the wind influences inside a dome end-to-end simulations as described above for radio telescopes and the airborne telescope would be appropriate. Main problem for the simulations are realistic data for the air pressure of the telescope inside the dome, which can be obtained by wind tunnel tests or measurements at existing facilities (see [28], see also the remarks on mirror segment supports in chapter X).

E. Simulations in the frequency domain

Before the availability of the powerful digital simulation tools, the structural engineers developed the power spectrum transfer method for the investigation of wind effects on buildings [29]. The method gives a good insight into the physical effects, and here is used for some comments based on a paper describing the analog techniques [30].

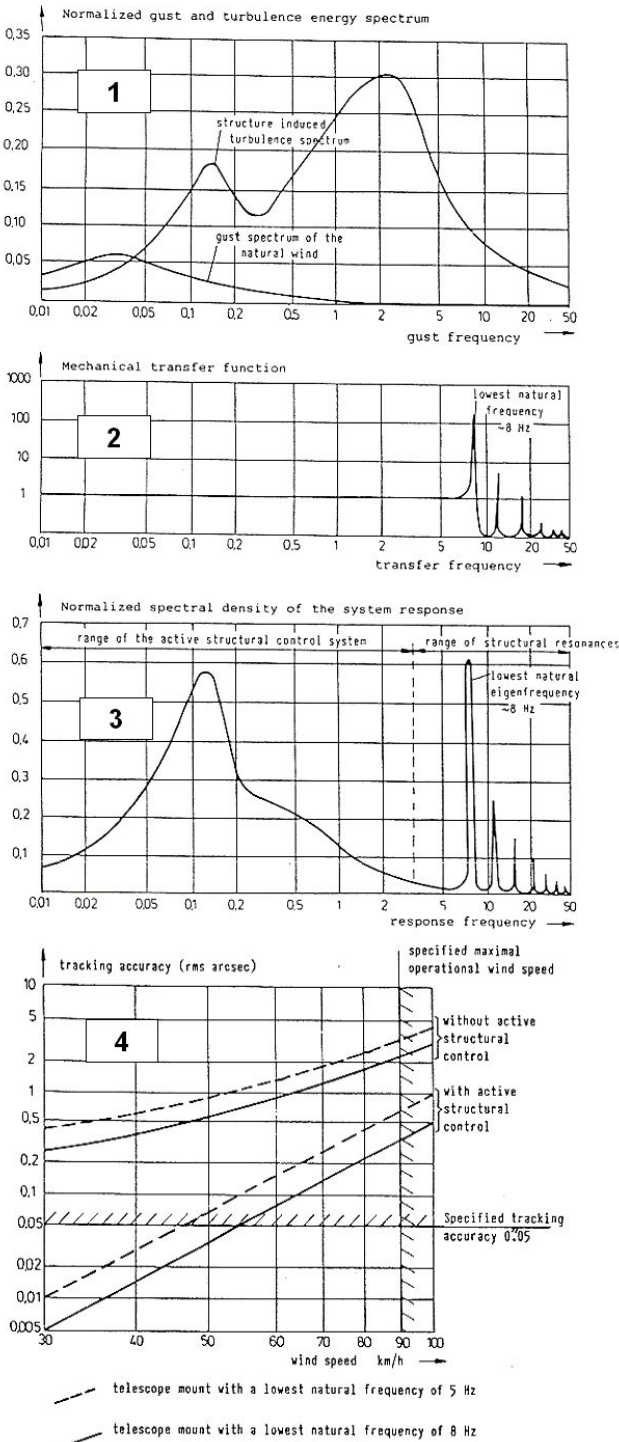


Figure XI-5 Power spectrum transfer method for wind loads on telescopes

Diagram 1 in Figure XI-5 shows the power spectrum of the wind according to Davenport [29], and the shift at higher frequencies caused by the influence of the dome and the telescope structure itself. Note that the maximum wind turbulence is at very low frequencies (0.04 Hz).

Diagram 2 shows the mechanical transfer function of the telescope structure. In the example case, the lowest resonance frequency was 8 Hz. Below the lowest frequency, the structure transfers dynamic wind loads directly to the foundation of the telescope (transfer function equal to 1).

Diagram 3 shows the response spectrum, equal to the superposition of the wind spectrum and the transfer function. Below the lowest resonance frequency, the telescope behavior is dominated by the “low frequency” wind gust. Above, the behavior is dominated by the resonance.

Diagram 4 shows the resulting pointing (tracking) error, obtained by cumulating the influence parameters of the response spectrum over the frequencies. The upper curves show the pointing error without active control at the low frequent. The lower curves show the results with the active control. The improvements are in the range of 1 to 2 orders of magnitude, which were confirmed with recent simulations.

For details of the method see [29] and [30].

XII. THERMAL SUBSYSTEMS

The thermal control issues are quite different to that of position control. The thermal behavior of an exposed telescope (Figure XII-1) is driven by solar radiation during the day, infrared radiation to the cold sky during night, and the moderate influence of convection by the surrounding air flow. Under clear sky conditions – typical for good astronomical observation conditions – these influences result in a day-night cycle for the temperatures in and around the telescope.

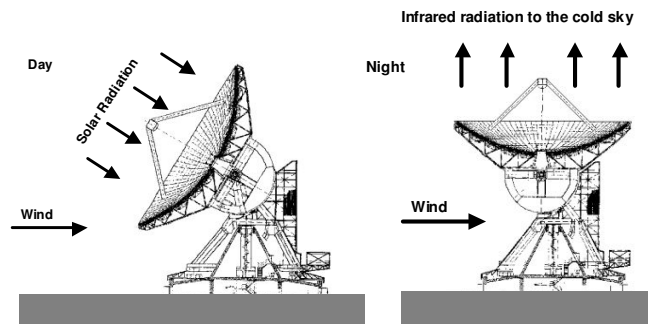


Figure XII-1 Thermal influences on a telescope

A. Thermal Subsystems for Radio Telescopes

Major issue of the thermal design of an exposed radio telescope is the handling of the temperature induced deformations. This is achieved by thermal protection, by thermal stable materials (carbonfiber composites), or by active correction of temperature induced deformations. In this chapter, the first method is addressed.



Figure XII-2 Thermal layout of the 30m MRT Spain reflector

Major task for the thermal subsystem is to achieve a uniform temperature distribution in the telescope structure. For a millimeter telescope made of steel, the uniformity must be typically ± 0.5 K. Absolute shifts of the mean temperature are tolerable, because they do not disturb the telescope optics. Major cause for temperature disturbances are differences in the thermal time constant of the telescope components. The thermal time constant depends on the ratio between the heat transfer coefficient of the component and its heat capacity (see [31]). The heat capacity is inherent to the structural mass of the component, the heat transfer coefficient can be influenced by insulation, surface treatment and forced air ventilation.

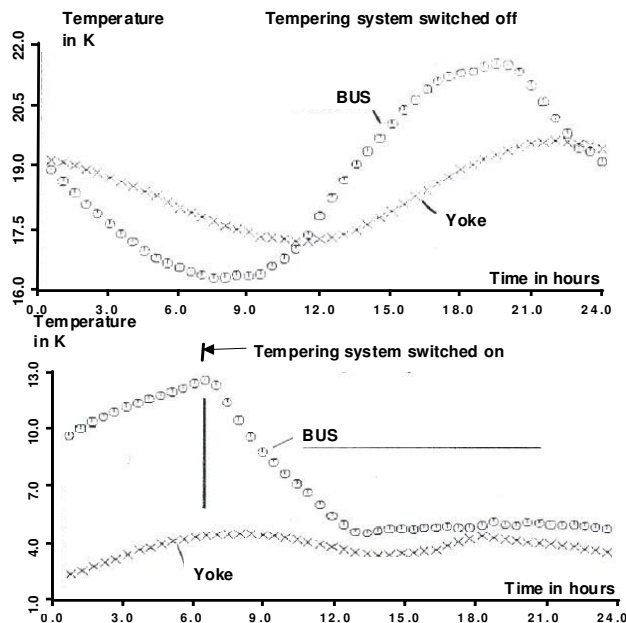


Figure XII-3 Measured temperature cycles 30m MRT Spain

Figure XII-3 shows the typical day-night cycles of the temperature of two thermal different components of the 30m MRT telescope in Spain. The reflector backup structure (BUS) of the MRT is rather filigree, but has a larger outer surface, compared with the yoke, which is very massive and has a small outer surface. Therefore, the thermal time con-

stant of the BUS is in the range of hours, that of the yoke in the range of days. This can be seen in the upper diagram of Figure XII-3. The BUS temperature follows nearly directly the course of the outside temperature, the yoke temperature with shift of several hours and with lower amplitudes. This behavior is the cause for temperature difference of several degrees between the BUS and the yoke, which introduces an astigmatic deformation of the main reflector in the range of millimeters. For the MRT, the problem was solved by a sophisticated “tempering” system, which cools down the BUS via the circulating air during the day and heats it up during the night. The lower diagram in Figure XII-3 shows the effectiveness of this system.

The tempering system of the MRT [10], is expensive even during operations due to its energy consumption for cooling and heating. Therefore, the LMT avoids the active cooling and heating [32] and relies on temperature monitoring and active correction using a thermal model as described in chapter VII. For radio telescopes with lower requirements, less effort for thermal control is needed, which includes a careful treatment of the thermal issues by adequate surface treatment (blank aluminum or white paint) and a FBC model for pointing (see e.g. [6]).

Finally some remarks on control issues. The requirements for active thermal systems are quite different than for the “fast” position control systems. Due to the long thermal time constants, the control cycles have frequencies in the range of 10^{-5} Hz, and the system reacts very slowly to changes of control parameters. This needs a very sophisticated commissioning strategy after installation of the system.

B. Thermal Subsystems for Earthbound Optical Telescopes

The requirements for thermal subsystems of optical telescopes are quite different to those of radio telescopes. First, the telescopes are normally used only during night, and protected against the sun during day by a dome; second, the deformation issues for the primary mirror are handled differently using iso-static principles [1], which reduce the deformation stability requirements for the “mirror cell” (as the BUS is called in optical telescopes). Therefore, the thermal issues of optical telescopes are dominated by “seeing”, disturbances introduced by convective fluctuations of the air in the optical path. The seeing is heavily influenced by the design of the dome, and thermal issues of dome design are widely discussed (e.g. [34]) and here not further commented.

C. Thermal Subsystems for Solar Telescopes

Thermal design is on its paramount for solar telescopes. The telescope must handle the incoming thermal energy without damages to the optical elements and receiving instruments. Therefore, normally a Gregorian arrangement of the optical elements is used, with a heat rejection device in the focus of the primary mirror, which reflects the incoming

thermal energy out of the optical beam. From the optical elements, only the primary is directly exposed to the sun.

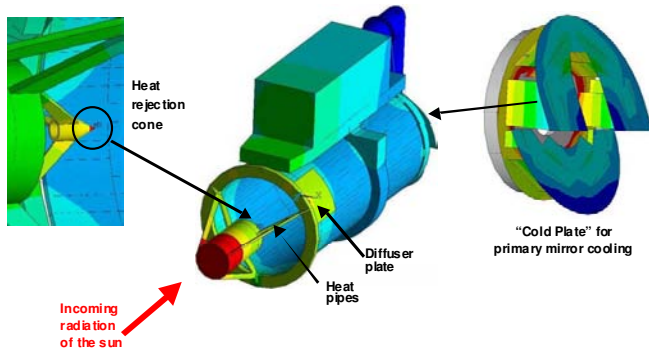


Figure XII-4 Thermal layout of a solar balloon telescope

Figure XII-4 shows the thermal situation⁹ of a solar balloon telescope [35]. The telescope will operate in great height (> 35 km) above the outer rim of Antarctica. The thermal system must operate completely passive, and only by radiation. Also the ice in Antarctica from the thermal system point of view - in the infrared range - is rather warm, and the radiation for the cooling is restricted to surfaces of 0° to 70° elevation. Heat transfer from the rejection cone to the diffuser plates is executed by “heat pipes”.

XIII. ERROR BUDGET AND FINAL PERFORMANCE

We discussed the influences and effects on the performance of telescopes from the mechatronic point of view. At some stage of the project, a summary must be made by the system engineer to get an overview on all the singular influences and their importance in the overall context. Most valuable in this regard are “error budget”. In the following the overall mechatronic aspects of error sources are discussed using the error budgets for the 50m LMT telescope in Mexico [8]. The errors are separated in surface and pointing errors as explained in chapter IX.

A. Surface error budgets

Figure XIII-1 in the first column gives the values of absolute, uncorrected surface errors. The second column gives the corrected errors values, the third column gives the correction method. The corrected error values are understood as root-mean-square (rms) errors of the 1 σ type. The errors are divided into errors due to environmental influences, manufacturing errors and alignment errors.

The LMT has an active surface, used for the correction of only two environmental effects, gravity and thermal deformations. The gravity deformations are corrected by the lookup tables (LTU), which are obtained from the finite element models and will be later improved by actual deformation measured at the erected telescope. The thermal deformations are corrected by temperature sensors and a thermal model (ThM). The maximal wind deformations are

just below the budget requirements, and not actively corrected.

The design approach included passive handling of the wind deformation. Identifying wind loads or wind induced deformations for active corrections of the reflector shape seems – due to the complexity of the wind loads in their spatial and time distribution much more complicated than for the temperature influences. The tables show the full, uncorrected wind induced surface errors.

Source and Type of Error	Uncorr.	Corr.	Corr. Tech.
Environmental Influences (steady-state)			
a) Gravity Deformations			
BUS	168	17	LUT
Panels	15	15	
b) Wind Deformations (10 m/sec)			
BUS	44	44	
Panels	6	6	
Subreflector lateral offset	14	14	
Subreflector defocus	6	6	
c) Thermal Deformations			
BUS	61	20	ThM
Panels	10	10	
Reflector Manufacturing			
Panels	15	15	
Subreflector	15	15	
Mechanical Alignment			
Panels	15	15	
Subreflector	15	15	
Margin		25	
Overall Surface Error Budget		69	

Figure XIII-1 Surface error budget of the 50m LMT (in $\mu\text{m rms}$)

B. Pointing error budgets

The pointing error budget in Figure XIII-2 follows the same conventions as the surface error budget with columns for uncorrected and corrected values, and one for the correction method. Also, the corrected error values are understood as of the 1 σ type and root square summed. But the table of influences is much more complex than that for the surface errors, because all the influences of the main axes mechanisms and position controllers were taken into account.

- The gravity deformations of the structures rotating in elevation are corrected via lookup tables. Remaining errors should be in the range of 2% of the absolute deformations. The alidade has no variable gravity deformations.

- The steady state components of the wind deformations are compensated by a modal observer algorithm based on inclinometer measurements as described in chapters VIII and IX. The estimate comprises the deformations of the alidade as well as the BUS. The remaining error corrections should be better than 10% of the absolute error.

- The pointing error induced by thermal deformations are handled similarly to the surface errors.

- The dynamic pointing errors due to the wind gusts consist of two components, one produced by the position controller, the other produced by dynamic deformations of the

⁹ Simulations executed with ANSYS thermal data package

structure above the angular position sensors. The values in the table are obtained from end-to-end simulations as described in chapter XI.

Source and Type of Error	Uncorr.	Corr.	Corr. Techn.
Environmental Influences (steady-state)			
a) Gravity Deformations			
Foundation	<<	<<	
Alidade	<<	<<	
BUS	< 10	(0,2)*	LuT
b) Wind Deformations (10 m/sec)			
Foundation	<<	<<	
Elevation	0,6	0	MoO
Cross Elevation	2,2	0,1	MoO
c) Thermal Deformations			
Foundation	<<	<<	
Alidade	< 1,0	(0,2)*	ThM
BUS	< 1,0	(0,2)*	ThM
d) FBC Uncertainty			
(*) : included in "FBC Uncertainty"		0,3	
Environmental Influences (Dynamic)			
Wind 10 m/sec :			
Gusts on Servo	0,3	0,3	
Gusts on Structure	0,2	0,2	
Mechanical Alignment			
Overall	5,0	0,5	ACM

Servo			
a) Sensors			
Encoder precision	0,07	0,07	
Encoder Couplings	0,07	0,07	
b) Actuators			
Backlash of drive units	5,00	0,03	DPT
Friction variation	1,00	0,30	DFF
Motor cogging	0,03	0,03	
Drive unbalance	0,03	0,03	
Servo amplifier offset and noise	0,03	0,03	
c) Servo Controller			
	0,03	0,03	
d) Servo Commands			
Velocity lag	5,00	0,02	DTG
Acceleration lag	3,00	0,05	DTG
Program track interpolation	0,02	0,02	
Time synchronisation	0,02	0,02	
Margin			
		0,30	
Overall Pointing Error			
		0,82	

Figure XIII-2 Pointing error budget of the 50m LMT (in arcsec rms)

- The alignment of the telescope axes during installation of the telescope may be not better than 5 arcsec. Corrections with a remaining error better than 10% of the alignment error are achieved with the astronomical calibration model.
- The servo system itself has four areas, where active corrections are used. First is the backlash of the main drives, which is corrected with a "drive pre tension" corrector DPT. The second is the friction at the azimuth wheels, which may be corrected by a disturbance feed forward feature DFF. The third and fourth are disturbances by the position commands as velocity and acceleration limits, which are handled by a dynamic trajectory generator DTG.

The tables give a good feeling for the magnitudes of the effects. In a conservative assessment, with all the active

features, an improvement of the absolute errors by more than one magnitude can be achieved for a 50m telescope.

C. Optical errors

The above discussed errors reflect the influence of the mechatronic system of the telescope on the overall performance. For the final result as an astronomical instrument, two other areas have to be addressed, which are errors induced by the optical system, such as imaging errors [36], and the quality of the receiving elements, such as cameras, feed horns etc. These problems belong to the observing astronomers itself.

XIV. COMMISSIONING

The final product will be only as good as team realizing it. The basic mechatronic system needs during commissioning close cooperation of structural, mechanical and control engineers (see Figure XIV-1). Later, during the first phases of operation, their close cooperation with the pioneering first astronomers in a "system optimization" phase is mandatory for ultimate results. Adequate time and resources must be allocated for this system optimization phase.



Figure XIV-1 SOFIA mechatronic commissioning team (Augsburg 2002)

XV. STRENGTH, STABILITY AND HAZARD ASPECTS OF TELESCOPES

Up to now performance was the main focus of this treatise. But, also stability and safety aspects are part of the production of a telescope, and they are mainly related to the mechatronic subsystem. Normally, the telescope structure is designed in regard of stiffness and dynamics, and strength and stability play a minor role in the design. But for larger telescopes, the verification of the strength and stability is needed. Until recently, the telescopes were small and understood as laboratory instruments. But now, people climb up the telescope during observation, and safety standards similar to buildings should be applied. Also structural fatigue is an issue, as collapses of large telescopes have been observed. For earthbound telescopes, all this should be handled according to the standard rules, and will here not be further discussed.

Regarding airworthiness issues of airborne telescopes see [14].

XVI. CONCLUSIONS

Structures, mechanics, and control are the backbone of each large telescope. Their design and implementation should follow mechatronic engineering rules complementary to the scientific approaches of the astronomers and opticians.

XVII. ACKNOWLEDGMENTS

This summary of the mechatronic aspects of telescopes is based on the 45 years of experience of the MAN telescope team in Mainz, Germany [37]. The author wants to express his reference to the founders of the telescope activities at MAN as well as to all the team members.

The author expresses his special appreciation to Wodek Gawronski of Jet Propulsion Laboratory, California Institute of Technology, Pasadena, CA, USA, who initiated the writing down of this overview.

REFERENCES

- [1] Kärcher, H.J., "Iso-static Mirror Supports vs. Homologue Reflectors – a Comparison", *Astronomical Structures and Mechanisms Technology*, Proc. SPIE 5495, 2004.
- [2] Kärcher, H.J., "Experience with the Design and Construction of Huge Telescope Pedestals", in 2nd Bäckaskog Workshop on Extremely Large Telescopes, Proc. SPIE 5382, 2003.
- [3] Kärcher, H.J., "Radioteleskope", in *Stahlbau-Kalender 2004*, Ernst & Sohn, Berlin 2004, S. 663-701, ISBN 3-433-01703-4
- [4] Kärcher, H.J., "Azimuth Axis Design for Huge Telescopes – an Update", in *Astronomical Structures and Mechanisms Technology*, Proc. SPIE 5495, 2004
- [5] Kärcher, H.J., "Das Große Millimeterwellen Teleskop auf dem Cerro la Negra in Mexiko", in *Der Stahlbau*, Heft 11, 2003
- [6] Kärcher, H.J., "Thermal effects on the pointing of the 32-m MERLIN radio telescope at Cambridge", *Astron. Astrophys.* 283, 1051-1057 (1994)
- [7] Kärcher, H.J., "Enhanced Pointing of Telescopes by Smart Structure Concepts based on Modal Observers", in *Smart Structures and Materials*, Proc. SPIE 3668, 1999
- [8] Kärcher, H.J., Baars, J.W.; "The Design of the Large Millimeter Telescope / Gran Telescopio Milimetrico (LMT/GTM)", in *Radio Telescopes*, SPIE 4015, 2000, S. 155 – 168
- [9] Parker, D.H., "The Green Bank Telescope Laser Metrology R&D Project: A Review and Bibliography", www.gb.nrao.edu/~rcreeger/GBTMetrology
- [10] Baars, J.W.M., Hooghoudt, B.G., Greve, A., Penalver, J., "Thermal Control of the IRAM 30-m Millimeter Radio Telescope," *Astronomy and Astrophysics*, 195, No. 1-2, pp 364-371
- [11] Schönhoff, U., Eisenträger, P., Wandner, K., Kärcher, H.J., Nordmann, R., "End-to-end Simulation of the Image Stability for the Airborne Telescope SOFIA", in *Airborne Telescope Systems*, Proc. SPIE 4014, 2000
- [12] Schedlinski, C., Link, M., "An Approach to Optimal Pick-up and Exciter Placement," 14th Int. Modal Analysis Conference, IMAC, Dearborn, MI, USA, 1996
- [13] Krabbe, A., Kärcher, H.J., "Preparing for First Light: The SOFIA Telescope", in *Astronomical Structures and Mechanisms Technology*, SPIE 5495, 2004
- [14] Kärcher, H.J., "Airborne Environment – a Challenge for Telescope Design," in *Airborne Telescope Systems*, SPIE 4014, 2000
- [15] Wandner, K., Kärcher, H.J., "The Pointing Control System of SOFIA," in *Airborne Telescope Systems*, SPIE 4014, 2000
- [16] Wandner, K., Gaiffe, T., Cottreau, Y., Faussot, N., Simonpietri, P., Lefevre, H., "Low Noise Fiber Optic Gyroscopes for the SOFIA Project," Symposium Gyro Technology, University of Stuttgart, Germany, 2000
- [17] Roddier, F. (ed), "Adaptive Optics in Astronomy", Cambridge University Press, ISBN 0 521 55375, 1999
- [18] Britt, R.B., "New 'Star' in Night Sky to Change View of Cosmos," www.space.com/sciencetech/astronomy/virtual_star
- [19] Kärcher, H.J., "System Background of MAN Pointing Calibration," internal report, MAN Technologie AG, Mainz, Germany, 2003
- [20] Meeks, M.L., Ball, J.A., Hull, A.B., "The Pointing Calibration of the Haystack Antenna", *IEEE Trans. Antennas Propagation* Vol. AP-16, No. 6, pp 746-751, 1968
- [21] Andersen, T., Ardeberg, A., Owner-Petersen, M., "Euro50 Design Study of a 50 m Adaptive Optics Telescope", Lund University, Sweden, 2003
- [22] Orfei, A., Morsiani, M., Zacciroli, G., Maccaferri, G., Roda, J., Flocchi, F., "Active surface system for the new Sardinia Radio Telescope", *Astronomical Structures and Mechanisms Technology*, Proc. SPIE 5495, 2004
- [23] Kärcher, H.J., "Experience with Wind Excited Mirror Vibrations", in 2nd Bäckaskog Workshop on Extremely Large Telescopes, Proc. SPIE 5382, 2003
- [24] Bonaccini, D., Ellerbroek, B., Ragazzoni, R. (ed.), "Advancement in adaptive optics", SPIE 5490, 2004
- [25] Gawronski, W. "Three Models of Wind-Gust Disturbance for the Analysis of Antenna Pointing Accuracy", IPN Progress Report 42-149, 2002
- [26] Eisenträger, P., Süß, M., "Verification of the Active Deformation Compensation System of the LMT/GTM by End-to-end Simulations", in *Radio Telescopes*, Proc. SPIE 4015, 2000, pp 488 – 497
- [27] Süß, M., Wandner, K., Kärcher, H.J., "Airborne Pointing and Pointing Improvement Strategy for SOFIA", in *Airborne Telescope Systems*, Proc. SPIE 4857, 2002
- [28] Smith, D.R., Avitabile, P., Gwaltney, G., Myung Cho, Sheehan, M., "Wind-induced structural response of a large telescope", in *Astronomical Structures and Mechanisms Technology*, Proc. SPIE 5495, 2004
- [29] Ruscheweyh, H., "Dynamische Windwirkung an Bauwerken", Bauverlag, Wiesbaden 1982
- [30] Kärcher, H.J., Nicklas, H., "Active structural control of very large telescopes", in *Active Telescope Systems*, Proc. SPIE 1114, 1989, pp 320 – 327
- [31] Kärcher, H.J., "Der Einfluss von Sonneneinstrahlung und Klima auf Teleskopstrukturen am Beispiel der Temperierungsanlage des MRT", *Universitätssternwarte Göttingen*, 1985
- [32] Kärcher, H.J., "Thermal Subsystem", LMT Project Technical Documentation, WP-22500-02, 2000
- [33] Kärcher, H.J., "Der Einsatz von CFK-Bauteilen bei Groß-Teleskopen und die Auswirkungen auf die Windverformung", *Universitätssternwarte Göttingen*, 1985
- [34] de Kock, M., Venter, S., "Design and Commissioning Experience of Salt Facility", in *Astronomical Structures and Mechanisms Technology*, SPIE 5495, 2004
- [35] Kärcher, H.J., "Concepts for a Lightweight Balloon Telescope for Solar Observation", in *Airborne Telescope Systems*, Proc. SPIE 4857, 2002
- [36] Wilson, R.N. "Reflecting Telescope Optics", 2 Vol., Springer, Berlin 2000
- [37] Kärcher, H.J., "45 years Antenna- and Telescopes from MAN Mainz", www.man.mt....